The Astrophysical Journal, 786:36 (8pp), 2014 May 1 doi:10.1088/0004-637X/786/1/36

LONGITUDINAL MAGNETOHYDRODYNAMICS OSCILLATIONS IN DISSIPATIVE, COOLING CORONAL LOOPS

K. S. Al-Ghafri, M. S. Ruderman, A. Williamson, and R. Erdélyi
Solar Physics and Space Plasma Research Centre (SP^{2}RC), University of Sheffield, Hicks Building, Hounsfield Road, Sheffield S3 7RH, UK;
app08ksa@sheffield.ac.uk, m.s.ruderman@sheffield.ac.uk, app09aw@sheffield.ac.uk, robertus@sheffield.ac.uk
Received 2012 October 29; accepted 2014 March 12; published 2014 April 14

ABSTRACT

This paper investigates the effect of cooling on standing slow magnetosonic waves in coronal magnetic loops. The damping mechanism taken into account is thermal conduction that is a viable candidate for dissipation of slow magnetosonic waves in coronal loops. In contrast to earlier studies, here we assume that the characteristic damping time due to thermal conduction is not small, but arbitrary, and can be of the order of the oscillation period, i.e., a temporally varying plasma is considered. The approximation of low-beta plasma enables us to neglect the magnetic field perturbation when studying longitudinal waves and consider, instead, a one-dimensional motion that allows a reliable first insight into the problem. The background plasma temperature is assumed to be decaying exponentially with time, with the characteristic cooling timescale much larger than the oscillation period. This assumption enables us to use the WKB method to study the evolution of the oscillation amplitude analytically. Using this method we obtain the equation governing the oscillation amplitude. The analytical expressions determining the wave properties are evaluated numerically to investigate the evolution of the oscillation frequency and amplitude with time. The results show that the oscillation period increases with time due to the effect of plasma cooling. The plasma cooling also amplifies the amplitude of oscillations in relatively cool coronal loops, whereas, for very hot coronal loop oscillations the damping rate is enhanced by the cooling. We find that the critical point for which the amplification becomes dominant over the damping is in the region of 4 MK. These theoretical results may serve as impetus for developing the tools of solar magneto-seismology in dynamic plasmas.

Key words: magnetohydrodynamics (MHD) – plasmas – Sun: corona – waves

1. INTRODUCTION

Standing slow MHD waves have been detected by SUMER in hot coronal loops with temperatures of the order of or larger than 6 MK (Wang et al. 2002, 2003; Taroyan et al. 2007). Further afield, intensity variations have been detected in various stellar environments. McAteer et al. (2005) and Anfinogentov et al. (2013) have interpreted these observational data as damped slow waves in stellar loops/arcades. An important and theoretically challenging property of these oscillations is their fast damping. To explain the observed fast damping various mechanisms have been proposed. Among them are thermal conduction, viscosity, radiation, and shock formation (Ofman & Wang 2002; De Moortel & Hood 2003; Mendoza-Briceño et al. 2004; Taroyan et al. 2005; Sigalotti et al. 2007; Bradshaw & Erdélyi 2008; Verwichte et al. 2008; Erdélyi et al. 2008). For a recent review on longitudinal oscillations, see, e.g., Wang (2011). It has been suggested that the dominant dissipative mechanism is likely thermal conduction. However, often it is found that thermal conduction alone is not sufficient to account for the observed damping (e.g., Sigalotti et al. 2007).

It is frequently observed that coronal loops are cooling with the characteristic cooling time of the order of a few oscillation periods (e.g., Aschwanden & Terradas 2008). Initially, the effect of cooling on coronal loop kink oscillations has been studied (Morton & Erdélyi 2009, 2010; Ruderman 2011a, 2011b). In particular, it was found that cooling causes the amplification of kink oscillations. Morton et al. (2010) investigated the effect of cooling on propagating MHD waves in a homogeneous plasma. They found that cooling causes the damping of propagating slow MHD waves. Erdélyi et al. (2011) studied the effect of cooling on propagating slow MHD waves in stratified coronal loops. They found that cooling and stratification cause a reduction in the damping rate. In a recent work by Al-Ghafri & Erdélyi (2013), the effect of cooling on standing slow MHD waves in coronal loops has been investigated.

Al-Ghafri & Erdélyi (2013) assumed that the cooling is weak with the characteristic cooling timescale much larger than the oscillation period. They also assumed that the thermal conduction is weak that restricted applicability to astrophysical plasmas. Then, they used the WKB method to study the evolution of the properties of longitudinal oscillations. The effects of cooling and thermal conduction on the oscillation amplitude were of the same order. In general, however, when thermal conduction is strong, it dominates the effect of cooling, so the account of cooling can provide only a small correction to the damping time. It is worth noting that there is one important exception. It is well known that the damping rate due to thermal conduction is a non-monotonic function of the thermal conduction coefficient (e.g., De Moortel & Hood 2003). When the thermal conduction coefficient increases, the damping rate first also increases, takes its maximum, and then starts to decrease and tends to zero as the thermal conduction coefficient tends to infinity. Hence, when thermal conduction is very strong, slow magnetosonic waves propagate almost without damping. Instead, when these waves propagate along the magnetic field, their phase speed reduces from the adiabatic to isothermal sound speed. This implies that cooling can substantially affect the damping rate not only when thermal conduction is weak but also when it is very strong. This work links these two disparate ideas into a continuous description of damping as a result of thermal conduction.

In this paper, we aim to study the effect of plasma cooling on the damping rate of slow standing MHD waves in coronal loops for *arbitrary* thermal conduction coefficient. The paper is organized as follows. In the next section, we formulate the

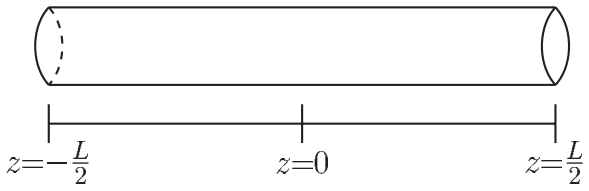

Figure 1. Coronal loop.

problem, and present the governing equations and boundary conditions. In Section 3, we carry out the analytical study of the problem using the WKB method. In Section 4, we present a numerical evaluation using the analytical solution. Section 5 contains the summary and discussion of the results and our conclusions.

2. THE MODEL AND GOVERNING EQUATIONS

We consider standing slow MHD waves in hot coronal magnetic loops. We model a magnetic loop as a straight homogeneous magnetic flux tube of length L with the constant magnetic field magnitude equal to B_0 (see Figure 1). We use the low-beta approximation applicable to solar coronal conditions. This enables us to use the rigid tube approximation when studying the propagation of longitudinal waves, and neglect the magnetic field perturbation. As a result, a standing slow MHD wave is a superposition of two sound waves propagating along the magnetic field in the opposite directions. We assume that the homogeneous plasma density, ρ_0, does not vary with time. On the other hand, both the plasma temperature, T_0, and pressure, p_0, are functions of time, the temperature dependence on time being given by

$$T_0 = T_{0i}\exp(-t/\tau_c), \tag{1}$$

where τ_c is the characteristic cooling timescale. We assume that cooling is slow, so $\epsilon = P/\tau_c \ll 1$, where P is the characteristic period of the loop oscillation. No mechanism for this cooling is suggested here, other than to note that the cooling is independent of the thermal conduction considered below. This assumption is made for the purposes of simplicity in the work performed here. Here, and in what follows, the subscript "i" indicates the value of a quantity at $t = 0$. The pressure is related to the temperature by the Clapeyron law,

$$p_0 = \frac{R}{\tilde{\mu}}\rho_0 T_0, \tag{2}$$

where $R = 8.3\times10^3\,\mathrm{m^2\,s^{-2}\,K^{-1}}$ is the gas constant and $\tilde{\mu}$ the mean molecular weight.

In our model the coefficient of thermal conduction along the magnetic field is given by $\kappa_\parallel = \kappa_0 T_0^{5/2}$, where κ_0 is a constant. The gravity is neglected.

Let us now perturb the governing MHD equations for the plasma motion by writing all variables in the form

$$f(z,t) = f_0(t) + f_1(z,t), \tag{3}$$

and introduce the dimensionless variables

$$\tilde{t} = \frac{t}{P},\quad \tilde{z} = \frac{z}{L},\quad \tilde{c}_s = \sqrt{\frac{T_0}{T_{0i}}},\quad \tilde{v}_1 = \frac{v_1}{c_{si}},\quad \tilde{T}_1 = \frac{T_1}{T_{0i}},$$
$$c_{si}^2 = \frac{\gamma R T_{0i}}{\tilde{\mu}}, \tag{4}$$

where the subscripts "0" and "1" represent the equilibrium and the perturbed quantities, respectively, z is the coordinate along the magnetic field, γ is the ratio of specific heats, v_1 and T_1 are the velocity and temperature perturbations, $\tilde{c}_s$ is the dimensionless sound speed, and we put $P = L/c_{si}$. In what follows we drop the tilde. We note at this point that while the discussion below takes place under the assumption of linear wave propagation, oscillatory loop systems similar to those investigated here contain nonlinear effects. This study, however, is strictly linear and as such aims to provide the foundation for future investigations into nonlinear wave propagation in appropriate solar and/or astrophysical plasmas.

Thus, the linearized perturbed MHD equations in a 1D system are

$$\frac{\partial\rho_1}{\partial t} + \frac{\partial v_1}{\partial z} = 0, \tag{5}$$

$$\frac{\partial v_1}{\partial t} = -\frac{1}{\gamma}\frac{\partial p_1}{\partial z}, \tag{6}$$

$$\left[\rho_1\frac{dT_0}{dt} + \frac{\partial T_1}{\partial t} + (\gamma-1)T_0\frac{\partial v_1}{\partial z}\right] = \sigma\, T_0^{5/2}\frac{\partial^2 T_1}{\partial z^2}, \tag{7}$$

$$p_1 = T_1 + T_0\rho_1, \tag{8}$$

where ρ_1 and p_1 are the density and pressure perturbations, and $v_1 \equiv v_{1z}$. The strength of thermal conduction is determined by the inverse Peclet number

$$\sigma = \frac{(\gamma-1)\tilde{\mu}\kappa_0 T_{0i}^{5/2}}{RL\sqrt{\gamma\, p_{0i}\,\rho_0}}. \tag{9}$$

For standard coronal conditions $\gamma = 5/3$, $\tilde{\mu} \approx 0.6$, and $\kappa_0 \approx 10^{-11}\,\mathrm{m^2\,s^{-1}\,K^{-5/2}}$. If we take $L = 100\,\mathrm{Mm}$ and $T_{0i} = 0.6$–$6\,\mathrm{MK}$ as typical coronal values then we obtain $0.007 \lesssim \sigma \lesssim 0.7$. At this point it must be noted that there is disagreement over the value of γ in the solar corona. Many previous studies have taken a value of 5/3 as a standard figure, however, recent observational investigations have found a value of $\gamma \approx 1.1$ in the corona (see e.g. Van Doorsselaere et al. 2011). However, if the value of γ were to be different from the 5/3 assumed here, the results derived below will not qualitatively change and the conclusions drawn will still be valid.

Al-Ghafri & Erdélyi (2013) have shown that the linearized system of governing Equations (5)–(8) can be reduced to one equation for v_1,

$$\frac{\partial^3 v_1}{\partial t^3} + \frac{7}{2}\epsilon\frac{\partial^2 v_1}{\partial t^2} - \frac{5}{2}\epsilon c_s^2\frac{\partial^2 v_1}{\partial z^2} - c_s^2\frac{\partial^3 v_1}{\partial t\partial z^2} - \epsilon\sigma c_s^5\frac{\partial^3 v_1}{\partial t\partial z^2}$$
$$- \sigma c_s^5\frac{\partial^4 v_1}{\partial t^2\partial z^2} + \frac{\sigma}{\gamma}c_s^7\frac{\partial^4 v_1}{\partial z^4} = 0. \tag{10}$$

Next, in order to set appropriate boundary conditions, we also need the relation between the velocity and temperature perturbation:

$$\frac{\partial^2 v_1}{\partial t^2} - \frac{c_s^2}{\gamma}\frac{\partial^2 v_1}{\partial z^2} + \epsilon\frac{\partial v_1}{\partial t} = -\frac{1}{\gamma}\left(\frac{\partial^2 T_1}{\partial t\partial z} + \epsilon\frac{\partial T_1}{\partial t}\right). \tag{11}$$

To study the damping of standing waves we need to impose the boundary conditions at $z = \pm1/2$. Since the loop ends are bounded by the dense photospheric plasma, we assume that the perturbation velocity vanishes at these ends,

$$v_1 = 0 \quad \text{at} \quad z = \pm1/2. \tag{12}$$

The thermal conduction drops dramatically at the photosphere. Hence, it is viable to assume that the loop is thermally insulated,

$$\frac{\partial T_1}{\partial z} = 0 \quad \text{at} \quad z = \pm 1/2. \tag{13}$$

Using Equation (11) we rewrite this boundary condition in terms of v_1,

$$\frac{\partial^2 v_1}{\partial t^2} - \frac{c_s^2}{\gamma}\frac{\partial^2 v_1}{\partial z^2} + \epsilon\frac{\partial v_1}{\partial t} = 0 \quad \text{at} \quad z = \pm 1/2. \tag{14}$$

Equations (10) and (11), and the boundary conditions (12) and (14) are used in the next section to study the damping of standing slow waves in cooling coronal loops.

3. ANALYTICAL SOLUTION

Let us introduce the "slow timescale" $t_1 = \epsilon t$. Now, we rewrite Equation (10) and the boundary condition (14) in terms of slow time,

$$\epsilon^3\frac{\partial^3 v_1}{\partial t_1^3} + \frac{7\epsilon^3}{2}\frac{\partial^2 v_1}{\partial t_1^2} - \frac{5\epsilon c_s^2}{2}\frac{\partial^2 v_1}{\partial z^2} - \epsilon c_s^2\frac{\partial^3 v_1}{\partial t_1 \partial z^2} - \epsilon^2\sigma c_s^5\frac{\partial^3 v_1}{\partial t_1 \partial z^2} - \epsilon^2\sigma c_s^5\frac{\partial^4 v_1}{\partial t_1^2 \partial z^2} + \frac{\sigma c_s^7}{\gamma}\frac{\partial^4 v_1}{\partial z^4} = 0, \tag{15}$$

$$\epsilon^2\frac{\partial^2 v_1}{\partial t_1^2} - \frac{c_s^2}{\gamma}\frac{\partial^2 v_1}{\partial z^2} + \epsilon^2\frac{\partial v_1}{\partial t_1} = 0 \quad \text{at} \quad z = \pm 1/2. \tag{16}$$

Then, we use the WKB method and look for the solution to Equation (15) with the boundary conditions (12) and (16) in the form

$$v_1(z, t_1) = Q(z, t_1)\exp(\mathrm{i}\epsilon^{-1}\Theta(t_1)). \tag{17}$$

Function Q is expanded in power series with respect to ϵ, i.e.,

$$Q = Q_0 + \epsilon Q_1 + \cdots. \tag{18}$$

3.1. Approximation of Geometrical Optics

Substituting Equations (17) and (18) into Equation (15) and the boundary conditions (12) and (16), we obtain in the leading-order approximation, often called the approximation of geometrical optics (e.g., Bender & Orszag 1991),

$$\frac{\partial^4 Q_0}{\partial z^4} + \frac{\gamma\omega}{c_s^2}\left(\omega - \frac{\mathrm{i}}{\sigma c_s^3}\right)\frac{\partial^2 Q_0}{\partial z^2} - \frac{\mathrm{i}\gamma\omega^3}{\sigma c_s^7}Q_0 = 0, \tag{19}$$

$$Q_0 = 0, \quad \frac{\partial^2 Q_0}{\partial z^2} = 0 \quad \text{at} \quad z = \pm 1/2, \tag{20}$$

where $\omega = d\Theta/dt_1$. The characteristic equation for Equation (19) is

$$\lambda^4 + \alpha\lambda^2 - \beta = 0, \tag{21}$$

where

$$\alpha = \gamma\frac{\omega^2}{c_s^2} - \mathrm{i}\frac{\gamma\omega}{\sigma c_s^5}, \qquad \beta = \mathrm{i}\frac{\gamma\omega^3}{\sigma c_s^7}. \tag{22}$$

The four roots of the bi-quadratic Equation (21) are $\lambda = \pm\mathrm{i}k_\pm$, where $k_\pm$ are given by

$$k_\pm = \sqrt{\frac{\alpha \pm \sqrt{\alpha^2 + 4\beta}}{2}}. \tag{23}$$

Then, the general solution to Equation (19) is

$$Q_0(z, t_1) = A_1\cos(k_+ z) + A_2\sin(k_+ z) + A_3\cos(k_- z) + A_4\sin(k_- z), \tag{24}$$

where A_i, $i = 1, \ldots, 4$ are arbitrary constants. Substituting Equation (24) in the boundary conditions (20) we obtain two systems of linear homogeneous algebraic equations,

$$\begin{aligned} A_1\cos(k_+/2) + A_3\cos(k_-/2) &= 0, \\ A_1 k_+^2\cos(k_+/2) + A_3 k_-^2\cos(k_-/2) &= 0, \end{aligned} \tag{25}$$

$$\begin{aligned} A_2\sin(k_+/2) + A_4\sin(k_-/2) &= 0, \\ A_2 k_+^2\sin(k_+/2) + A_4 k_-^2\sin(k_-/2) &= 0. \end{aligned} \tag{26}$$

The first system corresponds to symmetric and the second to anti-symmetric eigenmodes. Each of the two systems has a non-trivial solution only when its determinant is equal to zero. This condition gives the dispersion equation. Hence, the dispersion equation for symmetric eigenmodes is

$$(k_+^2 - k_-^2)\cos(k_+/2)\cos(k_-/2) = 0, \tag{27}$$

while it is

$$(k_+^2 - k_-^2)\sin(k_+/2)\sin(k_-/2) = 0, \tag{28}$$

for anti-symmetric eigenmodes. Since

$$(k_+^2 - k_-^2)^2 = \alpha^2 + 4\beta = \frac{\gamma^2\omega^2}{c_s^4}\left(\omega^2 - \frac{1}{\sigma^2 c_s^6} + 2\mathrm{i}\frac{(2-\gamma)\omega}{\gamma\sigma c_s^3}\right) \neq 0,$$

when $\omega \neq 0$, the dispersion equations for symmetric and anti-symmetric eigenmodes reduce to $k_\pm = \pi(2n-1)$ and $k_\pm = 2\pi n$, respectively, where $n = 1, 2, \ldots$. These two expressions can be unified to $k_\pm = \pi n$, where now odd n corresponds to symmetric and even to anti-symmetric eigenmodes. After simple algebra we can rewrite this equation in terms of ω,

$$\omega^3 - \mathrm{i}(\pi n)^2\sigma c_s^5\omega^2 - (\pi n)^2 c_s^2\omega + \mathrm{i}\frac{\sigma c_s^7}{\gamma}(\pi n)^4 = 0. \tag{29}$$

This dispersion equation is in agreement with that found by Field (1965), De Moortel & Hood (2003), and Erdélyi et al. (2011) in an appropriate limit. Note that, in the limit $\sigma \to 0$, i.e., if there is no thermal conduction, Equation (29) reduces to $\omega^2 = (\pi n c_s)^2$. In the case of very strong thermal conduction, i.e., when $\sigma \to \infty$, Equation (29) becomes $\omega^2 = (\pi n c_s)^2/\gamma$.

3.2. Approximation of Physical Optics

In what follows, we are only interested in the fundamental longitudinal mode corresponding to $n = 1$. Hence, either $k_+ = \pi$ or $k_- = \pi$. In both cases Equation (24) reduces to

$$Q_0(z, t_1) = A(t_1)\cos(\pi z), \tag{30}$$

where $A = A_1$ in the first case and $A = A_3$ in the second case. Now, we need to determine the function $A(t_1)$. To do this we proceed to the next order approximation, often called the approximation of physical optics (e.g., Bender & Orszag 1991). Substituting Equations (17) and (18) into Equation (15) and the

boundary conditions (12) and (16), and collecting terms of the order of ϵ, we obtain

$$\frac{\sigma}{\gamma}c_s^7\frac{\partial^4 Q_1}{\partial z^4}+\left(\sigma c_s^5\omega^2-\mathrm{i}c_s^2\omega\right)\frac{\partial^2 Q_1}{\partial z^2}-\mathrm{i}\omega^3 Q_1 = \left(\frac{7}{2}\omega^2+3\omega\frac{d\omega}{dt_1}\right)Q_0 + 3\omega^2\frac{\partial Q_0}{\partial t_1}+\left(\frac{5}{2}c_s^2+\mathrm{i}\sigma c_s^5\omega+\mathrm{i}\sigma c_s^5\frac{d\omega}{dt_1}\right)\frac{\partial^2 Q_0}{\partial z^2} + \left(c_s^2+2\mathrm{i}\sigma c_s^5\omega\right)\frac{\partial^3 Q_0}{\partial t_1\partial z^2}, \quad (31)$$

$$Q_1=0,\quad \frac{\partial^2 Q_1}{\partial z^2}=0 \quad \text{at} \quad z=\pm 1/2. \quad (32)$$

When deriving Equation (32) we have taken into account that $Q_0=0$ at $z=\pm 1/2$.

If we put the right-hand side of Equation (31) equal to zero, then we obtain the same eigenvalue problem as in the leading-order approximation. This problem has a non-trivial solution $Q_0 = A\cos(\pi z)$. This implies that boundary-value problem (31), Equation (32) has a solution only when the right-hand side of Equation (31) satisfies the compatibility condition, which is the condition that it is orthogonal to Q_0. This condition can be obtained by multiplying Equation (31) by Q_0, integrating with respect to z from $-1/2$ to $1/2$, and using the integration by parts and the boundary conditions (32). As a result we obtain

$$\int_{-1/2}^{1/2}\left[\left(\frac{7}{2}\omega^2+3\omega\frac{d\omega}{dt_1}\right)Q_0^2+3\omega^2 Q_0\frac{\partial Q_0}{\partial t_1} + \left(\frac{5}{2}c_s^2+\mathrm{i}\sigma c_s^5\omega+\mathrm{i}\sigma c_s^5\frac{d\omega}{dt_1}\right)Q_0\frac{\partial^2 Q_0}{\partial z^2} + \left(c_s^2+2\mathrm{i}\sigma c_s^5\omega\right)Q_0\frac{\partial^3 Q_0}{\partial t_1\partial z^2}\right]dz=0, \quad (33)$$

which gives the following equation for the evolution of the oscillation amplitude A,

$$2f(\omega,t_1)\frac{dA}{dt_1}+\left[\frac{\partial f}{\partial\omega}\frac{d\omega}{dt_1}+h(\omega,t_1)\right]A=0, \quad (34)$$

where

$$f(\omega,t_1)=3\omega^2-2\mathrm{i}\pi^2\sigma c_s^5\omega-\pi^2c_s^2, \quad (35)$$

$$h(\omega,t_1)=7\omega^2-2\mathrm{i}\pi^2\sigma c_s^5\omega-5\pi^2c_s^2. \quad (36)$$

Now we re-write the dispersion Equation (29) as

$$c_s^{-7}\omega^3-\mathrm{i}\pi^2\sigma c_s^{-2}\omega^2-\pi^2c_s^{-5}\omega+\mathrm{i}\frac{\sigma}{\gamma}\pi^4=0.$$

Differentiating this equation with respect to t_1, then multiplying by $2c_s^7$, and taking into account that $c_s=e^{-t_1/2}$ yields

$$2f\frac{d\omega}{dt_1}=-\omega h. \quad (37)$$

Substituting this result in Equation (34) and using Equation (35) we obtain

$$2f^2\frac{dA}{dt_1}=\pi^2c_s^2h\left(1+\mathrm{i}\sigma c_s^3\omega\right)A. \quad (38)$$

Integrating this equation we eventually arrive at

$$A(t_1)=A_0\exp\left(\pi^2\int_0^{t_1}\frac{c_s^2h(1+\mathrm{i}\sigma c_s^3\omega)}{2f^2}\,dt'\right), \quad (39)$$

where $A_0=A(0)$. Finally, the wave amplitude $a(t_1)$ is given by

$$a(t_1)=|A(t_1)|\exp\left(-\epsilon^{-1}\int_0^{t_1}\Im(\omega)\,dt'\right), \quad (40)$$

where $\Im$ indicates the imaginary part of a quantity.

It is instructive to compare the results derived in this section with those obtained by Al-Ghafri & Erdélyi (2013). These authors assumed that σ is small and took, as mentioned earlier, $\sigma=\mathcal{O}(\epsilon)$. For small σ we obtain from Equation (29)

$$\omega\approx\pi c_s+\mathrm{i}\frac{\sigma\pi^2c_s^5(\gamma-1)}{2\gamma}. \quad (41)$$

When calculating $A(t_1)$ we take $\omega\approx\pi c_s$ and neglect the term proportional to σ in the exponent and in the expressions for f and h. As a result we have

$$A(t_1)\approx A_0e^{t_1/4}. \quad (42)$$

Substituting Equations (41) and (42) in Equation (40) we arrive at

$$a(t)=A_0\exp\left[\left(\frac{\epsilon}{4}-\frac{\sigma\pi^2(\gamma-1)}{2\gamma}\right)t\right], \quad (43)$$

where we have also substituted $t_1=\epsilon t$. This expression coincides with that given by Al-Ghafri & Erdélyi (2013) (see their Equation (51)) if we take $n=0$ in the latter, which correspond to the fundamental mode, and neglect the small term proportional to ϵt^2 in the exponent.

In the next section, we use Equation (40) to analyze the temporary evolution of the oscillation amplitude.

4. NUMERICAL RESULTS

In this section, we use the analytical results obtained in the previous section to study the evolution of the periods and amplitudes of standing slow waves in cooling dynamical coronal loops. Since the analytical expressions are quite complex, we calculate the periods and amplitudes for typical coronal conditions numerically and plot the results. The oscillation period is equal to $2\pi/\omega_r$ where ω_r is the real part of the frequency, ω. The frequency has been calculated using Equation (29). At this point it is convenient to reiterate that the numerical work here is carried out with values typical to those of the solar corona. However, the general results will be applicable to stellar plasmas in a strictly qualitative manner.

Figure 2 displays the evolution of the oscillation period with time for various values of ϵ and the initial loop temperature. We see that the oscillation period increases with time due to cooling. This is an expected result because cooling decreases the phase speed. We can see that the effect is more pronounced in cooler loops.

The dependence of the oscillation amplitude on time for various values of ϵ and the initial loop temperature is displayed in Figure 3. We see that, in general, the oscillation amplitude decreases due to thermal conduction. When the loop temperature is not very high ($T\lesssim 5$ MK) cooling reduces the damping rate.

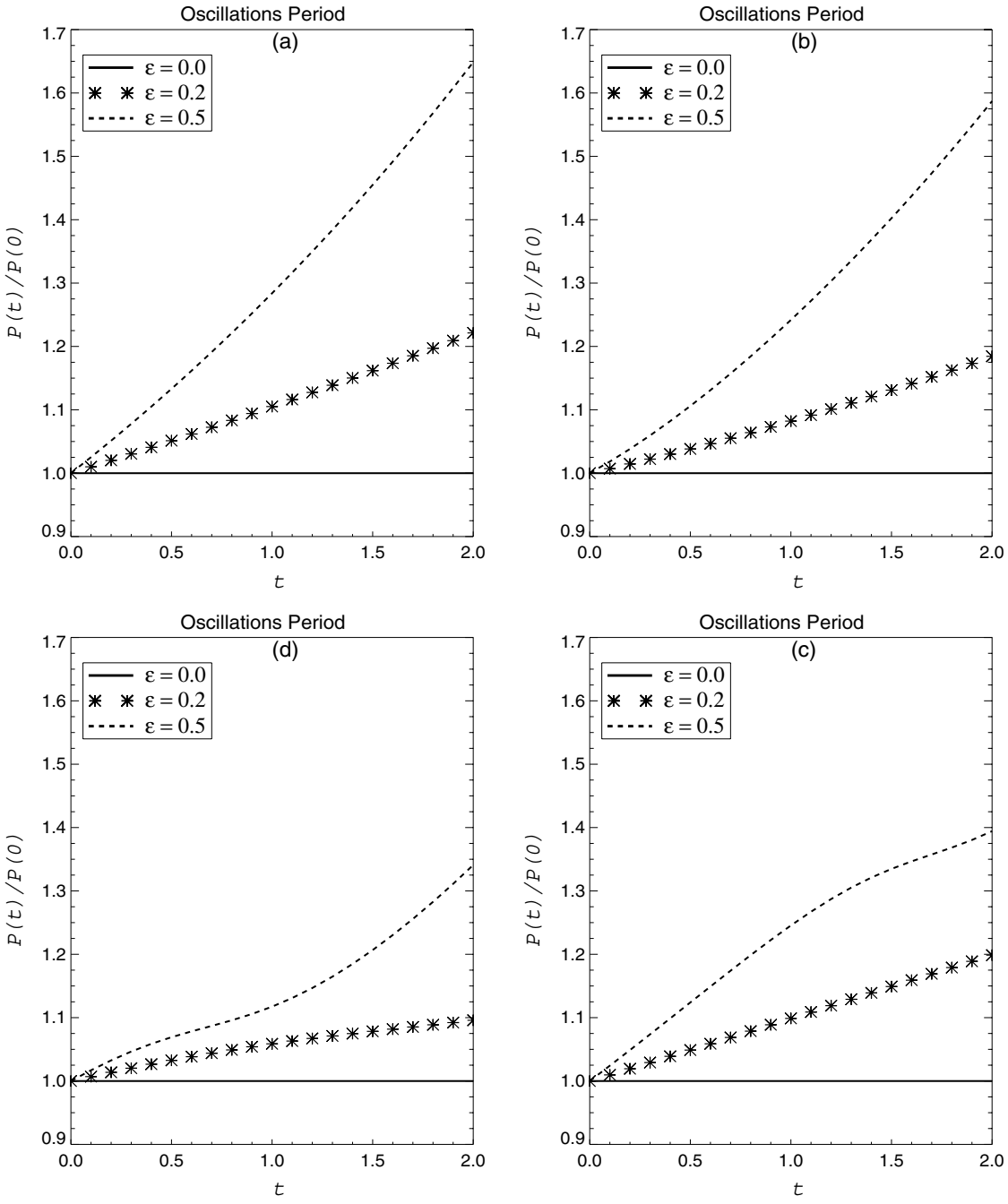

Figure 2. The dependence of the oscillation period on time for various values of ϵ and the loop temperature T. Recall that the time is measured in units of L/c_{si}. Panels (a), (b), (c), and (d) correspond to $T_{0i} = 0.6$ MK, $T_{0i} = 3$ MK, $T_{0i} = 6$ MK, and $T_{0i} = 10$ MK, respectively.

This feature is especially clearly seen in Figure 3(a). We can observe in this figure that the damping of oscillation is very weak. This result is consistent with the general conclusion that, in cool EUV loops ($T \lesssim 1$ MK) the thermal conduction is too weak to cause substantial damping of standing oscillations (e.g., Al-Ghafri & Erdélyi 2013). As a consequence, the amplification of oscillations due to cooling dominates damping due to thermal conduction, and the oscillation amplitude in cooling loops increases.

For a loop with larger temperatures ($T \gtrsim 3$ MK) even strong cooling ($\epsilon = 0.5$) cannot counter-balance damping due to thermal conductions, so it only can reduce the damping rate.

Figures 3(c) and (d) are especially interesting. We see in these figures that cooling enhances damping. The explanation of this effect is as follows. As we have already pointed out, the dependence of damping rate on the coefficient of thermal conduction and, consequently, on the loop temperature is not monotonic. It is clearly seen in Figure 3 that, in the absence of cooling, damping in a loop with $T = 10$ MK is weaker than that in a loop with $T = 6$ MK. This results is in agreement with the observation by Sigalotti et al. (2007) that slow standing oscillations of relatively cool loops ($T \sim 5$ MK) damp faster than those in very hot loops with $T \sim 10$ MK. Cooling decreases the temperature of the loop and, as a result, damping in the loop with the initial temperature 6 MK is becoming stronger.

It is now instructive to compare the results obtained in this paper with those obtained by Al-Ghafri & Erdélyi (2013). Figure 3(a) agrees very well with Figure 3(a) in Al-Ghafri &

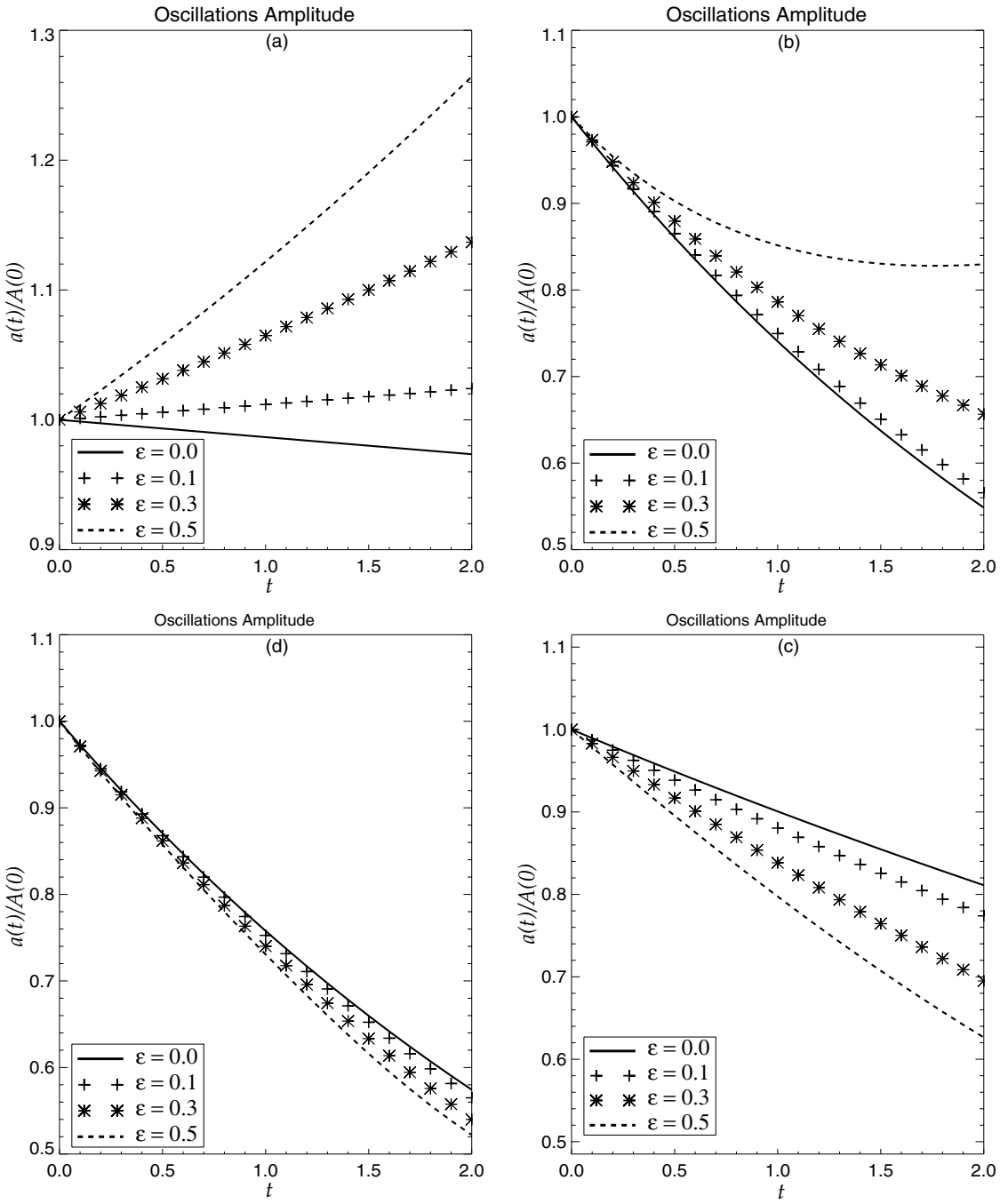

Figure 3. The dependence of the oscillation amplitude on time. Panels (a), (b), (c), and (d) correspond to $T_{0i} = 0.6$ MK ($\sigma = 0.0068$), $T_{0i} = 3$ MK ($\sigma = 0.17$), $T_{0i} = 6$ MK ($\sigma = 0.68$), and $T_{0i} = 10$ MK ($\sigma = 1.9$), respectively. The time is measured in units of L/c_{si}.

Erdélyi (2013). The agreement is fairly good for $T \lesssim 3$ MK. However, when the loop temperature increases further, the agreement is less clear. This discrepancy in not surprising because Al-Ghafri & Erdélyi (2013) assumed that damping is weak, which is less appropriate for sufficiently hot loops.

The results shown in Figure 3 are obtained for $\kappa_0 = 10^{-11}$. It is expedient to study the dependence of the damping rate on κ_0. Figure 4 shows the dependence of the oscillations amplitude on time for $\epsilon = 0.1$, $T_{0i} = 3$ MK, and various values of κ_0. As it can be expected, damping becomes stronger when κ_0 increases.

Figure 5 depicts the relation between the oscillation amplitude and the temperature for various values of ϵ at $t = 1$. The damping rate of coronal oscillations increases gradually, takes its maximum at the temperature ~4 MK, and then decreases onward.

It is worth studying what should be the cooling rate to compensate damping due to thermal condition and thus provide an undamped oscillation. These undamped longitudinal oscillations have yet to be directly observed, however, undamped fast kink MHD waves have already been detected by Aschwanden & Schrijver (2011). The theoretical results derived here do indicate that, with the recent improvements in observational equipment, undamped longitudinal oscillations should soon be detected.

In what follows, we consider the oscillation as undamped if $a(2) = 1$, i.e., if the oscillation amplitude at $t = 2$ is the same

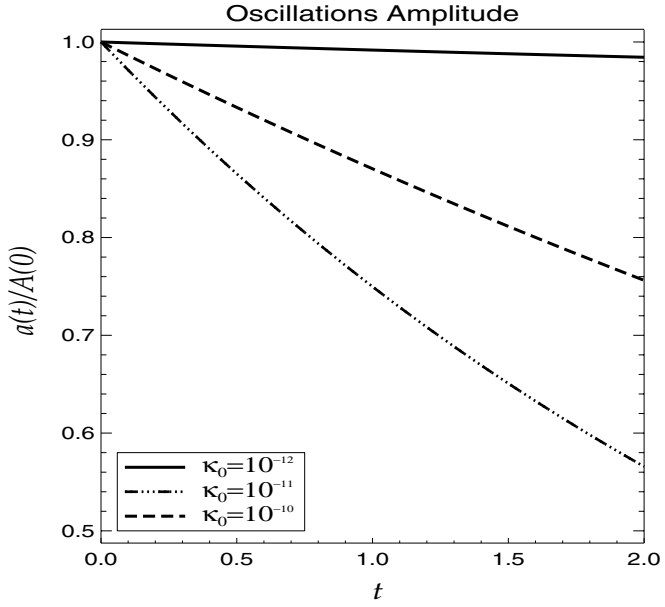

Figure 4. The dependence of the oscillation amplitude on time for $\epsilon = 0.1$, $T_{0i} = 3$ MK, and various values of κ_0. The time is measured in units of L/c_{si}.

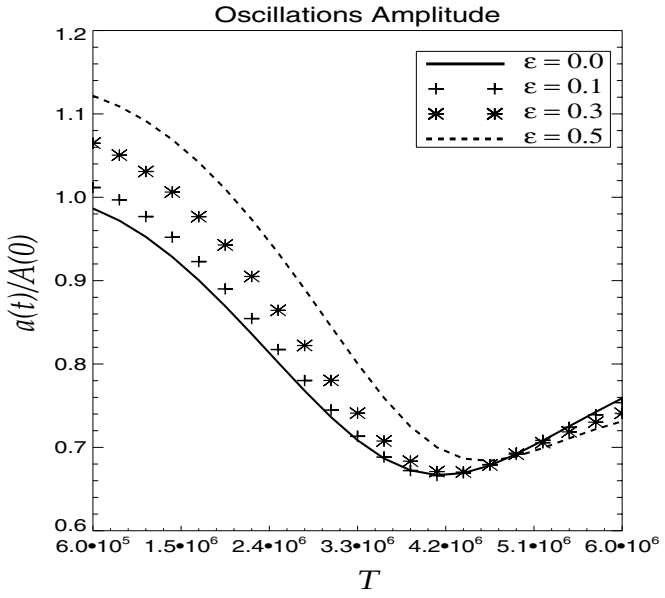

Figure 5. The dependence of the oscillation amplitude on temperature for $t = 1$, and various values of ϵ.

as at the initial moment of time. Since the damping rate due to thermal conduction is a function of the initial temperature, so is the cooling rate needed to compensate the damping. The cooling rate is defined by the parameter ϵ. Let us calculate the dependence of the value of ϵ needed to compensate the damping on the inverse Peclet number σ analytically using Equation (43) valid for weak damping, and numerically using Equation (40). The results of this calculation are shown in Figure 6. As it can be expected, the analytical and numerical solutions are very close for small values of σ, but they are sufficiently different for larger values of σ.

5. DISCUSSION AND CONCLUSION

In this paper, we have studied the effect of cooling of coronal loops on the damping of slow standing waves. We have used the low-beta plasma and rigid flux tube approximation, which

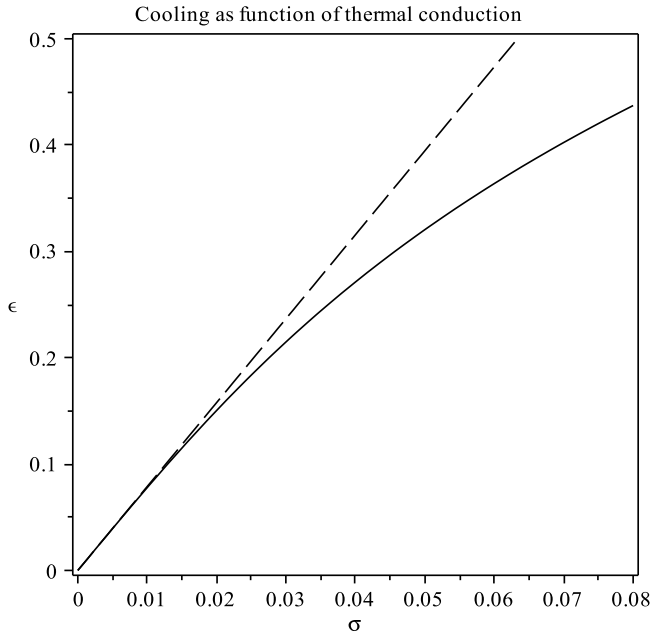

Figure 6. The required cooling rate to balance the thermal ratio (the inverse Peclet number) for $t = 2$, and $a(t) = 1$. The dashed and solid lines correspond to the analytical and numerical calculations, respectively.

enable us to disregard the magnetic field perturbation. As a result we have reduced the problem to studying one-dimensional standing acoustic waves. We have assumed that, due to cooling, the temperature in the loop decreases exponentially with the characteristic timescale τ_c, which is much longer than the characteristic oscillation period P, i.e., that we consider a temporally slowly varying plasma. The latter assumption has allowed us to use the WKB method with $\epsilon = P/\tau_c$ as a small parameter to model the damped oscillations. In the leading-order approximation of the WKB method, called the approximation of geometrical optics, we have derived the dispersion equation determining the instantaneous complex frequency of the loop oscillation. In the next order approximation, called the approximation of physical optics, we have obtained the equation determining the variation of oscillation amplitude with time.

We have used the analytical results to estimate the dependence of the oscillation period and amplitude on time numerically. We have obtained that cooling results in the increase of the oscillation period. This is an expected result because cooling causes the decrease of the sound speed, and the oscillation period is equal to the double time of the travel of a signal from one loop footpoint to the other. In not very hot loops (the temperature not exceeding ~5 MK) cooling reduces the damping rate due to thermal conduction. In cold loops with the temperature below ~1 MK the damping due to thermal conduction is very weak. As a result the effect of oscillation amplification dominates the damping and the oscillation amplitude increases with time. In hotter loops cooling cannot compete with damping and is able only to reduce the damping rate.

The damping rate is not monotonic function of the temperature. While it increases with the temperature in relative cold loops, the temperature increase in very hot loops leads to the decrease of the damping rate. As a result, in very hot loop with the temperature about 6 MK and higher cooling causes the damping enhancement.

In light of the results found here, as well as the observation of undamped fast MHD waves (see e.g. Aschwanden & Schrijver

2011; Wang et al. 2012), we expect that undamped slow MHD waves should not remain unobserved, especially inside cooler, <1 MK structures.

As briefly discussed in Section 2, the numerical models analyzed in this work are aimed specifically at solar coronal loops. However, by applying the analytical results, and the physical principles behind them, we can expect that the same temporal evolution will occur in more generalized, astrophysical plasmas, albeit with different quantitative values.

The authors are grateful to Science and Technology Facilities Council (STFC) for the financial support. K.S.A. acknowledges the financial support by the Ministry of Higher Education, Oman. M.S.R. acknowledges the support by a Royal Society Leverhulme Trust Senior Research Fellowship. R.E. is grateful to NSF, Hungary (OTKA, Ref. No. K83133), for the support received, and to M. Kéray for patient encouragement.

REFERENCES

Al-Ghafri, K. S., & Erdélyi, R. 2013, SoPh, 283, 413
Aschwanden, M. J., & Schrijver, C. J. 2011, ApJ, 736, 102
Aschwanden, M. J., & Terradas, J. 2008, ApJL, 686, L127
Anfinogentov, S., Nakariakov, V. M., Mathioudakis, M., Van Doorsselaere, T., & Kowalski, A. F. 2013, ApJ, 773, 156
Bender, C. M., & Orszag, S. A. 1991, Advanced Mathematical Methods for Scientists and Engineers (New York: Springer)
Bradshaw, S. J., & Erdélyi, R. 2008, A&A, 483, 301
De Moortel, I., & Hood, A. W. 2003, A&A, 408, 755
Erdélyi, R., Al-Ghafri, K. S., & Morton, R. J. 2011, SoPh, 272, 73
Erdélyi, R., Luna-Cardozo, M., & Mendoza-Briceño, C. A. 2008, SoPh, 252, 305
Field, G. 1965, ApJ, 142, 531
McAteer, R. T. J., Gallagher, P. T., Brown, D. S., et al. 2005, ApJ, 620, 1101
Mendoza-Briceño, C. A., Erdélyi, R., & Sigalotti, L. D. G. 2004, ApJ, 605, 493
Morton, R., & Erdélyi, R. 2009, ApJ, 707, 750
Morton, R., & Erdélyi, R. 2010, A&A, 519, A43
Morton, R., Hood, A. W., & Erdélyi, R. 2010, A&A, 512, A23
Ofman, L., & Wang, T. 2002, ApJL, 580, L85
Ruderman, M. S. 2011a, SoPh, 271, 41
Ruderman, M. S. 2011b, A&A, 534, A78
Sigalotti, L. D. G., Mendoza-Briceño, C. A., & Luna-Cardozo, M. 2007, SoPh, 246, 187
Taroyan, Y., Erdélyi, R., Doyle, J. G., & Bradshaw, S. J. 2005, A&A, 438, 713
Taroyan, Y., Erdélyi, R., Wang, T. J., & Bradshaw, S. J. 2007, ApJL, 659, L173
Van Doorsselaere, T., Wardle, N., Del Zanna, G., et al. 2011, ApJL, 727, L32
Verwichte, E., Haynes, M., Arber, T., & Brady, C. S. 2008, ApJ, 685, 1286
Wang, T. J. 2011, SSRv, 158, 397
Wang, T. J., Solanki, S. K., Curdt, W., Innes, D. E., & Dammasch, I. E. 2002, ApJL, 574, L101
Wang, T. J., Solanki, S. K., Innes, D. E., Curdt, W., & Marsch, E. 2003, A&A, 402, L17
Wang, T., Ofman, L., Davila, J. M., & Su, Y. 2012, ApJL, 751, L27